A simple scale height model of the electron density in Saturn's plasma disk

A. M. Persoon,[1] D. A. Gurnett,[1] W. S. Kurth,[1] and J. B. Groene[1]

Received 2 June 2006; revised 10 August 2006; accepted 21 August 2006; published 26 September 2006.

[1] A study of electron densities in Saturn's inner magnetosphere is presented using measurements of the upper hybrid resonance frequency obtained from the Radio and Plasma Wave Science (RPWS) instrument on the Cassini spacecraft. The study uses data from the first 16 months of operation in orbit around Saturn. The distribution of density data spans latitudes up to 20° and ranges from $3.6 \leq L \leq 8.6$. The results are compared to a simple centrifugal potential model for the plasma density. The measurements for $5 \leq L \leq 8.6$ yield a good fit to an equatorial electron density profile that varies as $n_0 = (51{,}880)\ L^{-4.1}$ cm^{-3} and a plasma scale height that varies as $H = (0.047)\ L^{1.8}$ R_S, where R_S is the radius of Saturn. The measurements for $L < 5$ are more variable, most likely due to plasma injection effects by Saturn's moon Enceladus which is a known source of neutral gas. A contour map of the electron densities derived from the centrifugal potential model is presented over the entire range of L values and latitudes analyzed, using cubic polynomials to represent the radial profiles of the equatorial electron density and the plasma scale height. **Citation:** Persoon, A. M., D. A. Gurnett, W. S. Kurth, and J. B. Groene (2006), A simple scale height model of the electron density in Saturn's plasma disk, *Geophys. Res. Lett.*, *33*, L18106, doi:10.1029/2006GL027090.

1. Introduction

[2] Several models of the spatial distribution of the plasma in Saturn's inner magnetosphere were developed using early plasma measurements acquired by the Pioneer 11 and Voyagers 1 and 2 spacecraft in 1979, 1980, and 1981 and remote sensing HST observations [*Richardson and Sittler*, 1990; *Richardson*, 1995, 1998; *Richardson and Jurac*, 2004]. These models were based on plasma measurements obtained during single flybys of Saturn, separated by many months. More recent plasma measurements have been made by the Cassini spacecraft, which was placed in orbit around Saturn on July 1, 2004. These include plasma composition and distribution function measurements from the Cassini Plasma Spectrometer (CAPS) instrument [*Young et al.*, 2005] and electron densities derived from the frequency of the upper hybrid resonance emissions detected by the Cassini Radio and Plasma Wave Science (RPWS) instrument [*Gurnett et al.*, 2004; *Moncuquet et al.*, 2005; *Persoon et al.*, 2005, 2006] and from the RPWS Langmuir probe instrument [*Wahlund et al.*, 2005]. In this paper, RPWS electron densities obtained over a 16-month interval from July 1, 2004 to October 30, 2005 are used to develop a simple model for the average plasma density in the inner magnetosphere of Saturn inside 8.6 saturnian radii (1 R_S = 60,268 km). For a discussion of the upper hybrid technique for determining the electron density and for previous results on equatorial electron densities at Saturn, see *Persoon et al.* [2005, 2006].

[3] The spatial distribution of RPWS upper hybrid measurements for the nineteen orbits used in this study is shown in Figure 1. More than 116,000 electron densities are derived from these upper hybrid measurements obtained over a range of L-shell values, $3.6 \leq L \leq 8.6$, where L refers to the McIlwain L-shell parameter [*McIlwain*, 1961], and spanning latitudes of +16 degrees to −20 degrees. Inside L = 3.6, there are few upper hybrid measurements because of spacecraft trajectory limitations. Outside L = 8.6, the upper hybrid emissions often become very irregular and weak, falling below background noise levels beyond ~10 R_S.

2. A Simple Plasma Density Model

[4] Since our main objective is to present a simple analytical model for the electron density, it is useful to give a brief derivation of the model. In the region of Saturn's magnetosphere beyond 2.3 R_S, centrifugal force is the dominant force acting on the co-rotating plasma [*Richardson and Sittler*, 1990]. In cylindrical coordinates, the centrifugal force is given by

$$F_c = m_i \rho \Omega^2, \tag{1}$$

where m_i is the ion mass, ρ is the perpendicular distance from the rotational axis of the planet and Ω is the rotation rate of Saturn. The potential energy of a particle in the co-rotating plasma can be found by integrating the negative of the centrifugal force along the ρ direction which gives,

$$W = -\frac{1}{2} m_i \rho^2 \Omega^2. \tag{2}$$

For our purposes it is convenient to convert to spherical coordinates using $\rho = r\cos\lambda$, where λ is the latitude and r is the radial distance from the center of the planet. Since Saturn's magnetic dipole axis is aligned almost exactly parallel to the rotational axis [*Smith et al.*, 1980], the magnetic field line in polar coordinates can be described by the equation $r = R_0 \cos^2\lambda$, where R_0 is the point at which the magnetic field line intersects the equatorial plane. By a series of substitutions, the potential energy of a particle moving along the dipole field line can be expressed in terms of the single variable λ

$$W = -\frac{1}{2} m_i \Omega^2 R_0^2 \cos^6 \lambda. \tag{3}$$

[1]Department of Physics and Astronomy, University of Iowa, Iowa City, Iowa, USA.

0094-8276/06/2006GL027090

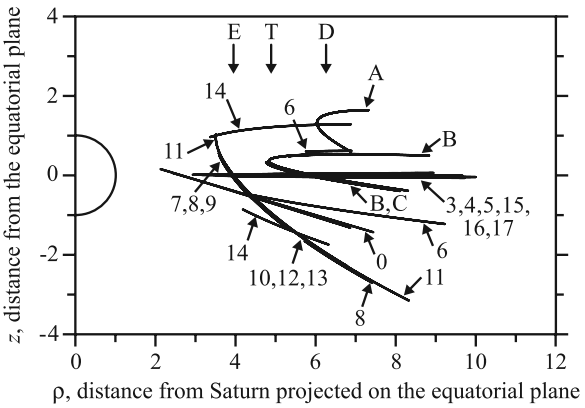

Figure 1. A meridian plane plot of the locations of the RPWS electron density measurements obtained between July 1, 2004 and October 30, 2005. The coordinate ρ is the perpendicular distance from Saturn's spin axis and z is the distance above/below the equatorial plane, both in saturnian radii. Each path of density measurements is labeled with the orbit number of the corresponding Cassini trajectory. The orbital radii of Saturn's moons Enceladus (E), Tethys (T) and Dione (D) are indicated by arrows at the top of the plot.

For our purposes it is useful to subtract the equatorial potential energy from the above equation so that the potential energy is zero at the equator, which gives

$$W = \frac{1}{2} m_i \Omega^2 R_0^2 \left(1 - \cos^6 \lambda\right). \tag{4}$$

From a well-known principle of equilibrium statistical mechanics, the number density is expected to vary as $n_i = n_{i0} \exp(-W/\kappa T_i)$, where n_{i0} is the density of the ith ion species at $\lambda = 0$, κ is Boltzmann's constant, and T_i is the temperature. From the charge neutrality condition, $n_e = \Sigma_i n_i$, it follows that the electron density can be written

$$n_e = \sum_i \alpha_i n_0 \exp\left[-\frac{m_i \Omega^2 R_0^2}{2\kappa T_i}\left(1 - \cos^6 \lambda\right)\right], \tag{5}$$

where $\alpha_i = n_{i0}/n_0$ is the fractional concentration of the ith ion species at the equator and n_0 is the total equatorial plasma density. The above equation can be simplified further by noting that the plasma scale height, H_i, is related to κT_i by $H_i^2 = 2\kappa T_i/3m_i\Omega^2$ [*Hill and Michel*, 1976]. For notational simplicity, it is convenient to write R_0 in terms of L using $R_0 = LR_S$, where R_S is one saturnian radius. The electron density is then given by the simple equation

$$n_e = \sum_i n_0 \alpha_i \exp\left[-\frac{1}{3}\frac{L^2}{H_i^2}\left(1 - \cos^6 \lambda\right)\right], \tag{6}$$

where, for notational simplicity, H_i is expressed in units of R_S. This expression is similar to the equation, $n_i = n_0 \exp[-(z/H)^2]$, developed by *Hill and Michel* [1976] and *Bagenal et al.* [1980] to describe the plasma distribution along Jupiter's magnetic field lines for small z.

[5] In Saturn's inner magnetosphere there are two dominant ion species, protons (H^+) and water group ions (W^+) [*Young et al.*, 2005]. Therefore, only two ion terms need to be considered in equation (6). From the analytical form of equation (6), it is evident that a plot of ($\ln n_e$) as a function of ($1 - \cos^6\lambda$) for a given L should consist of two asymptotic straight lines, one for each of the two ion species. To see if equation (6) provides a reasonable fit to the measured electron densities, the density measurements and the latitude of the spacecraft at the time of each density measurement were averaged in bins of $L \pm 0.2$, with each bin containing one averaged density value with its averaged latitude coordinate for the inbound pass and one averaged density value with its averaged latitude coordinate for the outbound pass, for each of the nineteen orbits used in this study. Plots of ($\ln n_e$) versus ($1 - \cos^6\lambda$) were then constructed for each L-shell value.

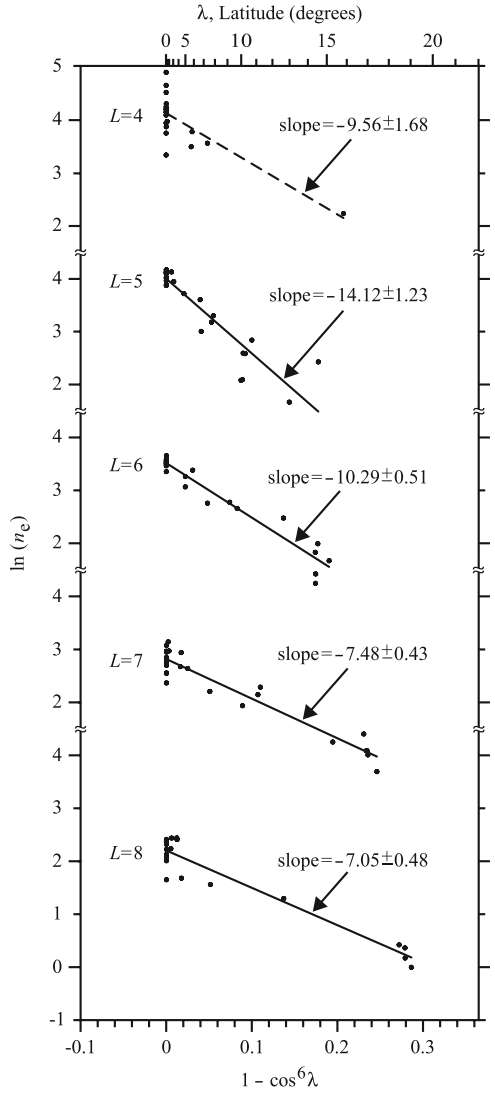

Figure 2. The natural logarithm of the measured electron densities, averaged in bins of $L \pm 0.2$ for five representative values of L, plotted as a function of the parameter ($1 - \cos^6\lambda$). The range of latitudes (in degrees) is given along the top axis. The plasma scale height H is derived from the slope of the best straight line fit and is given by $-(1/3)(L/H)^2$. The best fit line for $L = 4$ is poorly defined at the high-latitude end because of the lack of density measurements for $\lambda > 10°$ in this L-shell bin.

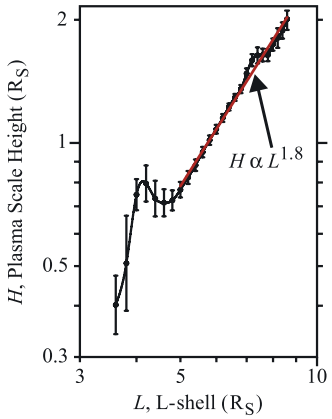

Figure 3. A plot of the plasma scale height derived from the slope of the best straight line fit for all density measurements plotted as a function of the natural logarithm of the electron density and the parameter $(1 - \cos^6\lambda)$, as shown in Figure 2. The best straight line fit through the scale height values for $5 \leq L \leq 8.6$ gives a power-law dependence of $L^{1.8}$. The solid black line represents a cubic spline fit through all of the data points.

Five representative plots are shown in Figure 2 for $L = 4$, 5, 6, 7, and 8. A single straight line provides a good fit to the data for each L-shell value although, for $L \leq 5$, there is more scatter in the distribution of the data points around the best fit line and fewer density measurements available at higher latitudes. The greater scatter in the density measurements for $L \leq 5$ is attributed to plasma sources in this region of Saturn's magnetosphere [*Persoon et al.*, 2005].

[6] Since the heavier water group ions are expected to be concentrated near the equator [*Young et al.*, 2005], the straight line fit in Figure 2 indicates that the plasma is dominated by water group ions. For the relatively low latitudes sampled in this study, $|\lambda| < 20°$, it is apparent that the spacecraft has not yet reached the high-latitude region where protons constitute a significant component of the ion population. A significant proton component would appear as a second asymptotic line at the higher latitudes. Note that this does not mean that no protons are present for $|\lambda| < 20°$. It simply means that the latitudinal distribution of the currently available measurements does not extend to sufficiently high latitudes to be able to resolve the proton contribution. From equation (6), it is easy to see that the plasma scale height H can be derived from the slope of the straight line fit for each L value and is given by $-(1/3)(L/H)^2$. The intercept of the straight line fit at $\lambda = 0$ gives the equatorial density n_0 at each L value.

[7] Using the results from the above fitting procedure, we next investigate how the parameters H and n_0 in equation (6) vary with L. As one can see from Figure 2, the magnitude of the slope of the best straight line fit through the data points decreases systematically with increasing L. The plasma scale height H, derived from the slope in all of the available L bins, is plotted as a function of L in Figure 3. For $L > 5$, the plasma scale height increases systematically with increasing radial distance and can be fit with good accuracy to the power-law equation $H = (0.047)\, L^{1.8}\, R_S$. The increase in the scale height with increasing radial distance implies that the temperature is increasing rapidly with increasing radial distance, consistent with the plasma temperature observations of *Moncuquet et al.* [2005], *Wahlund et al.* [2005], and *Young et al.* [2005].

[8] A corresponding plot of the equatorial electron density n_0 as a function of L is shown in Figure 4. For $L \geq 5$, the equatorial electron densities decrease systematically with increasing radial distance and can be fit with good accuracy to the inverse power law equation $n_0 = (51{,}880)(1/L)^{4.1}\text{cm}^{-3}$. These results can be compared to the source-free, centrifugal-driven outflow discussed by *Persoon et al.* [2005]. For a source-free expansion in which the frozen-field condition applies (BA = constant, where $B \sim (1/L)^3$), the total number of particles in a flux tube $n_0\, HL^3$ should be a constant. Using the above power-law dependences gives $n_0\, HL^3 \sim L^{0.7}$, which implies that plasma is being continually added to the plasma disk over a large region as it expands radially outward.

3. A Contour Plot of the Electron Density in the Meridian Plane

[9] In order to visualize the structure of Saturn's plasma disk, it is useful to construct a contour plot of the electron density in the meridian plane. In order to produce smooth contours, a cubic spline fit was used to provide a functional representation of n_0 and H as functions of L for $3.6 \leq L \leq 8.6$. These cubic spline fits are shown by the solid black lines through the data points in Figures 3 and 4. By making the appropriate substitutions for L and λ, equation (6) can then be used to compute the electron density at any arbitrary point (ρ, z) in the meridian plane. The contours of constant electron density are shown in Figure 5. This plot implicitly assumes azimuthal symmetry about Saturn's rotational axis and mirror symmetry about the equatorial plane.

[10] The maximum equatorial electron density is greater than 50 cm^{-3} out to 5.2 R_S. Beyond 5 R_S, the constant density contours are relatively smooth and the densities decrease slowly with increasing latitude and radial distance, consistent with a steady outward expansion of the plasma. Inside 5 R_S, there is a well-defined, field-aligned density enhancement at $L \approx 4.1$ and an abrupt decrease in the density inside $L \approx 4.1$.

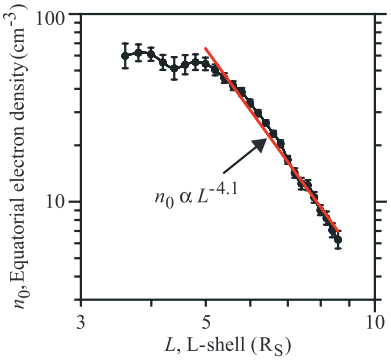

Figure 4. A plot of the equatorial densities derived from the y-intercept of the best straight line fit for all density measurements plotted as a function of the natural logarithm of the electron density and the parameter $(1 - \cos^6\lambda)$, as shown in Figure 2. The best straight line fit through the densities for $5 \leq L \leq 8.6$ gives an inverse power-law dependence of $L^{-4.1}$. The solid black line represents a cubic spline fit through all of the data points.

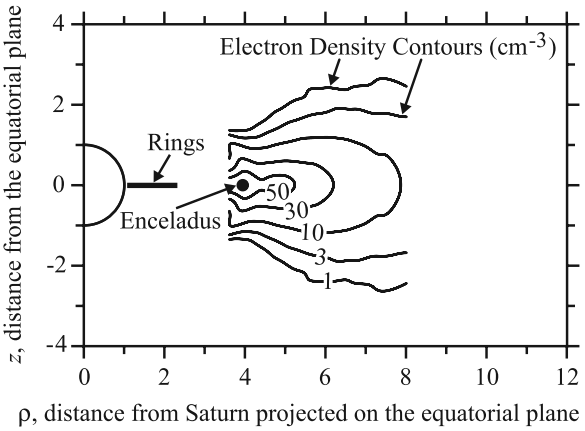

Figure 5. A contour plot of the electron density in Saturn's inner magnetosphere constructed from a simple exponential scale height model, where ρ is the perpendicular distance from Saturn's spin axis in the equatorial plane and z is the distance above/below the equatorial plane. All distances are given in saturnian radii.

This density enhancement is associated with a well-defined peak in the plasma scale height at $L \approx 4.1$ (see Figure 3). Note that the error bars are much larger in this region than for $L > 5$. The large error bars are indicative of large orbit-to-orbit density variations in this region, variations that have been previously noted by *Persoon et al.* [2005]. The sharp decrease in the density inside $L \approx 4$ is a consistent feature in earlier contour maps of the electron density in Saturn's magnetosphere [*Richardson and Sittler*, 1990; *Richardson*, 1995, 1998; *Richardson and Jurac*, 2004]. The density enhancement at $L \approx 4.1$ is very close to the orbit of Saturn's moon Enceladus, which is now known to be a significant source of neutral gases and plasma, specifically in the form of water group ions [*Dougherty et al.*, 2006; *Hansen et al.*, 2006; *Tokar et al.*, 2006; *Waite et al.*, 2006].

4. Conclusions

[11] An exponential scale height model is used to describe the electron density in the inner region of Saturn's magnetosphere. Using only a single ion term, the model provides a very good fit to the electron densities for $5 \leq L \leq 8.6$ and $|\lambda| \leq 20^\circ$ with only small orbit to orbit variations, typically less than ±25%. For this L value range, the equatorial electron density and the plasma scale height vary with L as $n_0 = (51{,}880)\ (1/L)^{4.1}$ cm^{-3} and $H = (0.047)\ L^{1.8}$ R_S. For an outward radial expansion in which the frozen-field condition applies, the total number of particles in a flux tube, $n_0 H L^3$, is found to vary as $L^{0.7}$, which implies that plasma is being continually added to the plasma disk as it expands. Inside $L = 5$, the electron density is more variable and has a well-defined enhancement at $L \approx 4.1$. This enhancement is most likely associated with the production of plasma from gases ejected by Saturn's moon Enceladus. There are no obvious density enhancements that might be related to other moons in the inner region of the magnetosphere.

[12] It is evident that the exponential scale height model with only one ion component provides a very good fit to the electron density for the range of latitudes and radial distances sampled. A second ion component could not be resolved, most likely due to the limited range of latitudes sampled, $|\lambda| \leq 20^\circ$. That a second straight line fit, indicative of the proton component, could not be resolved in the plot of (ln n_e) versus $(1 - \cos^6\lambda)$ does not mean that there are no protons present. It simply means that they are not dominant over a sufficiently large latitudinal range to be resolved in the plot of (ln n_e) versus $(1 - \cos^6\lambda)$. Eventually, as more data are accumulated at higher latitudes, it should be possible to resolve the proton component. Since we do not know the relative contribution to the electron density due to protons, caution must be exercised in interpreting the quantity that we have called the plasma scale height H in terms of the scale height of the water group ions, H_{W+}. The best that we can say from this study alone is that the scale height of the water group ions is less than the scale height obtained from the straight line fit, since protons are likely to be making a significant contribution to the electron density at the higher latitudes. In a separate study of ion scale heights by *Akalin et al.* [2006] based on an analysis of the dispersion of a whistler observed at $L = 6.49$ by Cassini, the proton concentration first reaches 50% at a latitude of 20°, which suggests that proton dominance in the plasma population is just beginning at the highest latitudes covered in this study. *Akalin et al.* [2006] also conclude that the scale height of the water group ions is $H_{W+} = 0.89$ R_S at $L = 6.49$. At the same L value (see Figure 3), the plasma scale height derived from our simple scale height model is $H = 1.2$ R_S, which suggests that the plasma scale height that we measure must be reduced by ~30% to give a comparable scale height for the water group ions.

[13] The simple exponential scale height model that we have used for the electron density is a steady-state model and has a number of shortcomings. It does not take into account the difference between the proton and water group ion temperatures and the anisotropy in the ion velocity distributions; it does not take into account the ambipolar electric field that arises due to charge separation; and it does not take into account gravitational forces. However, in the region near the equator, all of these effects are relatively small and the simple model gives a very good fit to the measured electron densities. Later in the Cassini mission, as the orbital inclination is increased to larger angles, we expect to obtain electron densities at much higher latitudes, where protons are expected to dominate. When these data are analyzed, it is likely that the modeling will have to be modified to take into account some of these effects.

[14] **Acknowledgments.** The authors would like to acknowledge useful discussions with Dave Young of Southwest Research Center, Ed Sittler of Goddard Space Flight Center, and Ferzan Akalin of the University of Iowa in the course of writing this paper. This research was supported by NASA through JPL contract 1224107.

References

Akalin, F., D. A. Gurnett, T. F. Averkamp, A. M. Persoon, O. Santolik, W. S. Kurth, and G. B. Hospodarsky (2006), The first whistler observed in the magnetosphere of Saturn, *Geophys. Res. Lett.*, doi:10.1029/2006GL027019, in press.

Bagenal, F., J. D. Sullivan, and G. L. Siscoe (1980), Spatial distribution of plasma in the Io torus, *Geophys. Res. Lett.*, *7*, 41–44.

Dougherty, M. K., K. K. Khurana, F. M. Neubauer, C. T. Russell, J. Saur, J. S. Leisner, and M. E. Burton (2006), Identification of a dynamic atmosphere at Enceladus with the Cassini magnetometer, *Science*, *311*, 1406–1409.

Gurnett, D. A., et al. (2004), The Cassini radio and plasma wave investigation, *Space Sci. Rev.*, *114*, 395–463.

Hansen, C. J., L. Esposito, A. I. F. Stewart, J. Colwell, A. Hendrix, W. Pryor, D. Shemansky, and R. West (2006), Enceladus' water vapor plume, *Science*, *311*, 1422–1425.

Hill, T. W., and F. C. Michel (1976), Heavy ions from the Galilean satellites and the centrifugal distortion of the Jovian magnetosphere, *J. Geophys. Res.*, *81*, 4561–4565.

McIlwain, C. E. (1961), Coordinates for mapping the distribution of magnetically trapped particles, *J. Geophys. Res.*, *66*, 3681–3691.

Moncuquet, M., A. Lecacheux, N. Meyer-Vernet, B. Cecconi, and W. S. Kurth (2005), Quasi thermal noise spectroscopy in the inner magnetosphere of Saturn with Cassini/RPWS: Electron temperatures and density, *Geophys. Res. Lett.*, *32*, L20S07, doi:10.1029/2005GL022648.

Persoon, A. M., D. A. Gurnett, W. S. Kurth, G. B. Hospodarsky, J. B. Groene, P. Canu, and M. K. Dougherty (2005), Equatorial electron density measurements in Saturn's inner magnetosphere, *Geophys. Res. Lett.*, *32*, L23105, doi:10.1029/2005GL024294.

Persoon, A. M., D. A. Gurnett, W. S. Kurth, G. B. Hospodarsky, J. B. Groene, P. Canu, and M. K. Dougherty (2006), An electron density model for Saturn's inner magnetosphere, in *Planetary Radio Emissions VI*, edited by H. O. Rucker, W. S. Kurth, and G. Mann, pp. 81–91, Osterreichisch. Akad. der Wissensch., Vienna.

Richardson, J. D. (1995), An extended plasma model for Saturn, *Geophys. Res. Lett.*, *22*, 1177–1180.

Richardson, J. D. (1998), Thermal plasma and neutral gas in Saturn's magnetosphere, *Rev. Geophys.*, *36*, 501–524.

Richardson, J. D., and S. Jurac (2004), A self-consistent model of plasma and neutrals at Saturn: The ion tori, *Geophys. Res. Lett.*, *31*, L24803, doi:10.1029/2004GL020959.

Richardson, J. D., and E. C. Sittler Jr. (1990), A plasma density model for Saturn based on Voyager observations, *J. Geophys. Res.*, *95*, 12,019–12,031.

Smith, E. J., et al. (1980), Saturn's magnetosphere and its interaction with the solar wind, *J. Geophys. Res.*, *85*, 5655–5674.

Tokar, R. L., et al. (2006), The interaction of the atmosphere of Enceladus with Saturn's plasma, *Science*, *311*, 1409–1412.

Wahlund, J.-E., et al. (2005), The inner magnetosphere of Saturn: Cassini RPWS cold plasma results from the first encounter, *Geophys. Res. Lett.*, *32*, L20S09, doi:10.1029/2005GL022699.

Waite, J.H., Jr., et al. (2006), The atmospheric plume of Enceladus as observed by the Cassini ion neutral mass spectrometer, *Science*, *311*, 1419–1422.

Young, D. T., et al. (2005), Composition and dynamics of plasma in Saturn's magnetosphere, *Science*, *307*, 1262–1266.

J. B. Groene, D. A. Gurnett, W. S. Kurth, and A. M. Persoon, Department of Physics and Astronomy, University of Iowa, Iowa City, IA 52242, USA. (joseph-groene@uiowa.edu; donald-gurnett@uiowa.edu; william-kurth@uiowa.edu; ann-persoon@uiowa.edu)